

Reionisation, chemical enrichment and seed black holes from the first stars: is Population III important?

M. Ricotti and J.P. Ostriker

Institute of Astronomy, Madingley Road, Cambridge CB3 0HA
ricotti@ast.cam.ac.uk, jpo@ast.cam.ac.uk

Accepted —. Received —; in original form 10 December 2002

ABSTRACT

We investigate the effects of a top-heavy stellar initial mass function on the reionisation history of the intergalactic medium (IGM). We use cosmological simulations that include self-consistently the feedback from ionising radiation, H₂ dissociating radiation and supernova (SN) explosions. We run a set of simulations to check the numerical convergence and the effect of mechanical energy input from SNe. In agreement with other studies we find that it is difficult to reionise the IGM at $z_{\text{rei}} > 10$ with stellar sources even after making extreme assumptions. If star formation in $10^9 M_{\odot}$ galaxies is not suppressed by SN explosions, the optical depth to Thomson scattering is $\tau_e \lesssim 0.13$. If we allow for the normal energy input from SNe or if pair-instability SNe are dominant, we find $\tau_e \lesssim 0.09$. Assuming normal yields for the first stars (population III), the mean metallicity of the IGM is already $Z/Z_{\odot} = 2 \times 10^{-3}$ ($10^{-3} < Z/Z_{\odot} < 1$ in overdense regions) when the IGM mean ionisation fraction is less than 10%. For these reasons population III stars cannot contribute significantly to reionisation unless the mechanical energy input from SNe is greatly reduced and either the metal yield or the mixing efficiency is reduced by a factor of 10^3 . Both problems have a solution if population III stars collapse to black holes. This can happen if, having masses $M_* < 130 M_{\odot}$, they are characterised by heavy element fall-back or if, having masses $M_* > 260 M_{\odot}$, they collapse directly onto black holes without exploding as SNe. If metal-poor stars are initially important and collapse to black holes is the typical outcome, then the secondary emission of ionising radiation from accretion on SN induced seed black holes, might be more important than the primary emission.

We also develop a semianalytic code to study how τ_e is sensitive to cosmological parameters finding essentially the same results. Neglecting feedback effects, we find simple relationships for τ_e as a function of the power spectrum spectral index and the emission efficiency of ionising radiation for cold dark matter and warm dark matter cosmologies. Surprisingly, we estimate that a warm dark matter scenario (with particle mass of 1.25 keV) reduces τ_e by only approximately 10%.

Key words: cosmology: theory, dark matter – galaxies: dwarf, formation, haloes – methods: numerical

1 INTRODUCTION

It is widely believed that the earliest generations of very low metallicity stars would have been far more effective than normal stars in reionising the universe, so much so that they could account for the large optical depth to Thomson scattering, $\tau_e = 0.17 \pm 0.04$, measured by the WMAP satellite (Bennett et al. 2003; Kogut et al. 2003). The main reason for this expectation is that the stellar initial mass function (IMF) is thought to be tipped towards high masses for $Z/Z_{\odot} \ll 10^{-4}$. But there are two byproducts which are likely to follow from this scenario. The same stars, which are efficient UV producers, will die as supernovae (SNe), the explosions heating the surroundings and inhibiting further star formation (“negative feedback”), and the metals ejected in these explosions will contaminate

the high density regions, rapidly bringing the metallicity up to a level where such stars cannot form. We argue that, while it is possible to evade these strictures, it is very difficult to do so unless this early generation ends its life primarily *via* implosion to black holes rather than explosion as supernovae, and that in the former case the secondary effects of ionising radiation from accretion onto the formed seed black holes may dominate over the primary UV from the first generation stars.

In this discussion we are focusing on the period $15 < z < 25$ when the haloes within which star formation would occur are small and gas cooling is initially via H₂ (Couchman & Rees 1986; Ostriker & Gnedin 1996). The later phase, responsible for the more complete reionisation of the universe as attested to by the Sloan

arXiv:astro-ph/0310331v3 14 Mar 2004

Digital Sky Survey (SDSS) quasars at $6 < z < 7$ (Becker et al. 2001; Fan et al. 2003), is fairly well understood and can easily be accounted for by a relatively normal population II. For a Salpeter mass function of population II stars in the mass range $1M_{\odot} \leq M_{*} \leq 100M_{\odot}$, and an escape fraction of UV photons from the forming galaxies to the IGM of $\langle f_{\text{esc}} \rangle = 20 - 50\%$, Gnedin (2000); Ciardi et al. (2003); Ricotti (2003a); Chiu et al. (2003) among others, find little difficulty in matching the QSO-determined ionisation history using standard stellar interiors theory and cosmological models. The two epochs of ionisation might have been distinct, as proposed by Cen (2003b), or there may have been an extended period of partial ionisation with a gradual transition to the epoch observed in quasars. If the IGM had a sudden transition from neutral to completely ionised, the measured optical depth $\tau_e = 0.17$ corresponds to a redshift of reionisation $z_{\text{rei}} = 17$ for the best fit Λ CDM cosmological model measured by WMAP (Spergel et al. 2003).

The large τ_e measured by WMAP implies that an additional source of ionising radiation is important at high-redshift. Two categories of sources have been considered in previous studies: (i) stellar or AGN sources, forming at $z \lesssim 40$ in the first galaxies (e.g., Cen 2003a; Wyithe & Loeb 2003; Somerville & Livio 2003; Ciardi et al. 2003; Sokasian et al. 2003) or (ii) exotic (unknown) sources such as decaying neutrinos (e.g., Sciama 1982; Hansen & Haiman 2004), super-heavy dark matter decay at recombination (Bean et al. 2003) or primordial BHs, either *via* evaporation (Guedens et al. 2002) or *via* accretion (Gnedin et al. 1995). In this paper (paper I) we study the early reionisation of the IGM by the first stars (population III). In two companion papers (paper IIa and paper IIb, Ricotti & Ostriker 2003; Ricotti, Ostriker, & Gnedin 2004) we study the partial ionisation by a putative X-ray background produced by mass accretion on seed BHs formed in the first galaxies.

Several groups have studied, using analytical calculations (e.g., Uehara et al. 1996; Larson 1998; Nakamura & Umemura 1999) or numerical simulations (e.g., Abel et al. 2002; Bromm et al. 1999), star formation in a metal-free gas. Most groups agree (but see Omukai & Palla 2003, for a more conservative point of view) that the first population of stars was probably massive, with typical mass of about $100 M_{\odot}$. The stellar IMF in the early universe is unknown but it is expected to be top-heavy or bimodal (Nakamura & Umemura 2001). It seems natural therefore that at high-redshift the emissivity of ionising radiation was larger than $\epsilon_{\text{UV}} \approx 1.3 \times 10^{-4}$ found for a Salpeter IMF. If all stars were massive ($M_{*} \gtrsim 10 M_{\odot}$), the emission efficiency of ionising radiation would be a factor of 10-20 larger than for the Salpeter IMF. During their lifetime massive stars convert a little less than half of their hydrogen into helium. The efficiency of thermonuclear reactions for the p-p chain is about 7 Mev per hydrogen atom. If we assume that all the energy liberated is emitted in ionising photons we obtain a theoretical upper limit for the UV emission efficiency $\epsilon_{\text{UV}}^{\text{max}} \lesssim 2 - 3 \times 10^{-3}$ (cf., Miralda-Escudé 2003). The maximum emission efficiency $\epsilon_{\text{UV}}^{\text{max}}$ can be obtained only if low-mass stars do not form and if all the ionising radiation can escape from the molecular clouds and the diffuse ISM of the host galaxy. Here ϵ_{UV} is the ratio of energy density of the ionising radiation field to the gas rest-mass energy density converted into stars ($\rho_{*}c^2$). Thus, $\epsilon_{\text{UV}} = (\overline{h_p\nu}/m_Hc^2)N_{\text{UV}}^{*}$, where N_{UV}^{*} is the emitted number of ionising photons (with mean energy $\overline{h_p\nu}$) per baryon converted into stars. At first glance, the enhanced efficiency of UV production from population III stars seems to be the natural explanation for the WMAP result. But as noted earlier there are

several issues that need to be addressed that make such a model difficult to achieve:

- Complete reionisation at increasingly high redshift requires a larger number of ionising photons per baryon. The recombination rate of hydrogen is large and the fraction of radiation escaping each galaxy is likely to be less than unity.

- The efficiency of star formation in small-mass haloes ($M_{\text{dm}} < 10^8 M_{\odot}$) is regulated by radiative feedback effects (i.e., star formation is reduced as a result of gas heating by UV, winds and SNe produced by star formation) and, according to cosmological simulations (Ricotti et al. 2002a,b), these galaxies cannot reionise the IGM. The simulations have shown that even assuming a top-heavy IMF, the star formation is strongly suppressed and the mean stellar mass in small-mass galaxies decreases. The simulation results agree with observations of the smaller-mass galaxies (dwarf spheroidal galaxies) in the Local Group that show the same large mass-to-light ratios (Ricotti 2003b).

- Later forming galaxies with masses $M_{\text{dm}} \gtrsim 10^9 M_{\odot}$ have a larger star formation efficiency and their stars could reionise the IGM. But the enhanced energy injection by SN explosions due to a top-heavy IMF would also reduce star formation in larger galaxies. If the energy of the SNe is normal ($E_{51} = E/[10^{51} \text{erg}] = 1$), the SN energy input for a top-heavy IMF would be larger than for a Salpeter IMF. Some massive stars are known to explode as hypernovae with energies $E_{51} \gg 1$. Supermassive stars with masses $140M_{\odot} < M_{*} < 260 M_{\odot}$ are thought to end their lives with an explosion (pair-instability SN) that does not leave any remnant. The explosion energy of pair-instability SNe (PIS) is proportional to their mass and is typically $E_{51} \gtrsim 100$.

- SN explosions eject metals into the ISM and IGM. The transition from a top-heavy IMF to a Salpeter IMF is thought to depend on the gas metallicity. If the metallicity is $Z \gtrsim 10^{-4} - 10^{-5} Z_{\odot}$ (Omukai 2000; Bromm et al. 2001; Schneider et al. 2002) the gas can cool more efficiently and to lower temperatures, allowing fragmentation and the formation of small-mass stars. The importance of population III stars for reionisation depends on how long metal-free gas is present in protogalaxies. This issue is difficult to address because it requires a good understanding of the mixing and transport processes of the heavy elements, but metals produced by SNe will clearly lead to an environment in which a top-heavy mass function no longer exists (e.g., see Wada & Venkatesan 2003). The only ways to avoid contamination that we have thought of are two: (i) have such efficient ejection of metals from star forming regions that lower density regions are contaminated before higher density ones ($d \ln Z/Z_{\odot}/d \ln \langle \rho \rangle < 0$) or (ii) have such inefficient local mixing that effective homogenisation is delayed for $0.5 - 1$ Gyrs, $\sim 5 - 10$ local dynamical times. We will return to these possibilities later.

This paper is organised as follows. In § 2 we show, using order of magnitude estimates, that a large τ_e favours a scenario in which a large fraction of the first massive stars collapse into primordial massive BHs. In § 3 we show the results of a set of cosmological simulations with radiative transfer. We focus on the effects of the limited mass resolution of the simulations and feedback from SN explosions. In § 4 we use a semianalytic calculation to estimate the effect of cosmological parameters on τ_e . In § 5 we present our conclusions.

2 BH-FORMING OR PAIR-INSTABILITY SUPERNOVAE?

In this section we use simple arguments to estimate the number of ionising photons needed to reionise the IGM. Since, conventionally, the massive stars that produce ionising radiation end their lives as SN explosions and BHs, we estimate the number density of metals and relic BHs expected given the redshift of reionisation (or τ_e). We show how the observed metallicity of the IGM and ISM in galaxies and the demographics of supermassive black holes (SMBH) at $z = 0$ can put some loose constraints on the IMF of the first stars. We find that it is very difficult to reionise the universe at high redshift without strongly contaminating it with metals. These calculations admittedly rely on simplistic assumptions but are useful to show the problems related with each scenario.

Assuming ionisation equilibrium we have,

$$\frac{dn_{\text{ph}}}{dt} \sim \frac{n_{\text{ph}}}{t_{\text{H}}} \sim \frac{\bar{n}_e}{\langle t_{\text{rec}} \rangle}, \quad (1)$$

where n_{ph} is the number density of ionising photons, \bar{n}_e is the mean electron number density, t_{H} is the Hubble time and $\langle t_{\text{rec}} \rangle = (\alpha_B n_e C_{\text{HII}})^{-1}$ is the mean recombination time inside the H II regions. The recombination and the Hubble times are, respectively,

$$\langle t_{\text{rec}} \rangle \sim 1.7 \text{Gyr} \left(\frac{\Omega_b h^2}{0.02} \right) \left(\frac{1+z}{7} \right)^{-3} C_{\text{HII}}^{-1}, \quad (2)$$

$$t_{\text{H}} \sim 1 \text{Gyr} \left(\frac{1+z}{7} \right)^{-1.5} \left(\frac{h}{0.7} \right)^{-1}, \quad (3)$$

where $C_{\text{HII}} = \langle n_{\text{HII}}^2 \rangle / \langle n_{\text{HII}} \rangle^2$ is the mean effective clumping factor of the ionised gas. The number of ionising photons emitted per hydrogen atom (also counting the number of recombinations per Hubble time) sufficient to fully reionise the IGM at redshift z_{rei} is given approximately by

$$N_{\text{ph}} \equiv \frac{n_{\text{ph}}}{n_{\text{H}}} \sim \max(t_{\text{H}} / \langle t_{\text{rec}} \rangle, 1) \sim \max([(1+z_{\text{rei}})/14]^{1.5} C_{\text{HII}}, 1), \quad (4)$$

where n_{H} is the mean hydrogen density. Assuming sudden reionisation at redshift $z_{\text{rei}} > (14C_{\text{HII}}^{-2/3} - 1)$ and neglecting the redshift dependence of the clumping factor, we have $N_{\text{ph}} \propto (1+z_{\text{rei}})^{1.5}$. The optical depth to Thomson scattering is given by

$$\tau_e = c\sigma_T \int dt n_e \sim 0.069 \frac{\Omega_b h}{\Omega_0^{1/2}} \int dz (1+z)^{1/2} \langle x_e \rangle_{\text{M}}, \quad (5)$$

where $\langle x_e \rangle_{\text{M}}$ is the mass weighted electron fraction. Assuming a sudden reionisation at redshift z_{rei} we have $\tau_e \propto (1+z_{\text{rei}})^{1.5}$, that has the same redshift dependence of N_{ph} . Therefore, in the case we neglect the redshift dependence of the clumping factor in equation (4), we find that N_{ph} is proportional to τ_e . A similar relationship was found by Oh et al. (2003) that, owing to the cancellation of the electron density in equation (5), also find the following expression:

$$N_{\text{ph}} = \frac{\tau_e}{n_{\text{H}} \langle t_{\text{rec}} \rangle c\sigma_T} \sim 10 \left(\frac{\tau_e}{0.1} \right), \quad (6)$$

that it is independent of redshift. The results of numerical simulations, presented in § 3.2, will show that this expression is not very accurate. A better agreement can be obtained using the equation

$$N_{\text{ph}} \sim 10 \left(\frac{\tau_e}{0.1} \right)^4, \quad (7)$$

that has been empirically derived from the simulations. The reason for this result is that the mean effective clumping factor inside the

H II regions it is not constant with redshift because it depends on the spatial distribution of the sources that are responsible for reionisation. The effective clumping factor, C_{HII} , is larger for reionisation at higher redshift because the sources, being more numerous and with smaller mean luminosity, must ionise first a large fraction of the dense filaments in which they are located. In the following calculations we use equation (6) because we want to use the most conservative assumption on the number of ionising photons N_{ph} . Using equation (7) would only change the exponent of τ_e from unity to four in the following relationships of this section.

If the massive stars that produce ionising radiation end their lives exploding as SNe and eject most of their mass enriched with heavy elements, the metal yield, Y , of a star population is approximately proportional to the number of ionising photons emitted, independently of the assumed IMF (e.g., Madau & Shull 1996). Using the population synthesis model STARBURST (Leitherer et al. 1999), we found that a population of stars with metallicity $Z \gtrsim 0.05 Z_{\odot}$ (population II) has a yield

$$Y = 15g Z_{\odot} \left(\frac{\epsilon_{\text{UV}}}{2 \times 10^{-3}} \right), \quad (8)$$

where $0.3 < g < 2$ depends weakly on the metallicity and ϵ_{UV} is the efficiency of ionising radiation emission from stars. As noted in the introduction, the maximum efficiency for thermonuclear reactions is $\epsilon_{\text{UV}}^{\text{max}} \lesssim E_{\text{p-p}} / m_{\text{H}} c^2 \lesssim 2 - 3 \times 10^{-3}$, where $E_{\text{p-p}}$ is the mean energy per nucleon emitted in form of ionising radiation. In this calculation we have assumed that population III stars during their lifetime are able to convert half of their hydrogen into helium and that they are hot enough to emit all their energy into ionising photons (cf., Miralda-Escudé 2003). The yield of population III is very uncertain. The main uncertainty comes from the unknown fraction of their stellar mass and metals that implodes into a black hole. In the following paragraph we will show that, if population III stars have “normal” yields (neglecting that a substantial fraction of their mass and metals is locked into the black hole remnant) they cannot produce the large τ_e measured by WMAP without a production of metals that is not consistent with the observed metallicities in the IGM and ISM.

The emissivity of ionising photons by massive stars is

$$\epsilon_{\text{UV}} \simeq X (1.36 \times 10^{-8}) N_{\text{UV}}^*,$$

where $X = \bar{h\nu} / 13.6 \text{eV} \approx 2 - 3$ is the mean energy of H I ionising photons and N_{UV}^* is the number of ionising photons per baryon converted into stars. If f_* is the fraction of baryons converted into stars we have $N_{\text{ph}} \equiv N_{\text{UV}}^* f_*$.

Let’s assume that massive population III stars have the same yields as massive population II stars. Since the total metal production is $Z = Y f_*$, using equation (8), we have

$$f_* = 6.8 \times 10^{-6} \left(\frac{2 \times 10^{-3}}{\epsilon_{\text{UV}}} \right) X N_{\text{ph}} \quad \text{and} \quad (9)$$

$$Z = (1g \times 10^{-4} Z_{\odot}) X N_{\text{ph}}. \quad (10)$$

The fraction of baryons that needs to be converted into stars to get a given τ_e can be estimated using equation (6) and using $X = 3$:

$$f_* \sim 2 \times 10^{-4} \left(\frac{2 \times 10^{-3}}{\epsilon_{\text{UV}}} \right) \left(\frac{\tau_e}{0.1} \right).$$

This relationship shows that, if the IMF is top-heavy, a smaller fraction of baryons needs to collapse into stars. We can also estimate the mean star fraction of galaxies $f_*^{\text{gal}} = f_* / f_{\text{coll}}$, where f_{coll} is the fraction of baryons in virialised DM haloes. At $z = 16$, most

of the collapsed baryons are in small-mass galaxies. The mass fraction of DM haloes with mass $M_{\text{dm}} < 10^8 M_{\odot}$ is $\Omega_{\text{dm}} \sim 1.74\%$ and, $\Omega_{\text{dm}} \sim 0.05\%$ in haloes with mass $M_{\text{dm}} > 10^8 M_{\odot}$. If we assume that the baryons follow the DM ($f_{\text{coll}} = \Omega_{\text{dm}}$), the fraction of gas converted into stars must be

$$f_*^{\text{gal}} \sim \begin{cases} 40\% \left(\frac{2 \times 10^{-3}}{\epsilon_{\text{UV}}} \right) \left(\frac{\tau_e}{0.1} \right) & \text{if } M_{\text{dm}} > 10^8 M_{\odot} \\ 1\% \left(\frac{2 \times 10^{-3}}{\epsilon_{\text{UV}}} \right) \left(\frac{\tau_e}{0.1} \right) & \text{if } M_{\text{dm}} < 10^8 M_{\odot}. \end{cases} \quad (11)$$

If galaxies in small-mass haloes do not contribute to reionisation, the efficiency of star formation in larger galaxies needs to be approximately 30 – 50 %, which is perhaps larger than the efficiency estimated for globular clusters. If small-mass galaxies contributed significantly to reionisation, then their efficiency of gas conversion into stars must be larger than 1 – 2 %. Assuming a “closed box” chemical evolution model for the galaxy, the ISM metallicity is

$$Z_{\text{ISM}} = Y f_*^{\text{gal}} = \begin{cases} 6g Z_{\odot} \left(\frac{\tau_e}{0.1} \right) & \text{if } M_{\text{dm}} > 10^8 M_{\odot} \\ 0.15g Z_{\odot} \left(\frac{\tau_e}{0.1} \right) & \text{if } M_{\text{dm}} < 10^8 M_{\odot}. \end{cases} \quad (12)$$

These metallicities are far too large when compared to the metallicities of the oldest star clusters known: old globular clusters that typically have $[m/H] = -1.5$ (e.g., Vandenberg et al. 1996) and dwarf spheroidal clusters that have $-2.5 < [m/H] < -1$ (e.g., Mateo 1998). To match observations all but 10^{-2} to 10^{-3} of the metals would need to have been ejected. With such a large *in situ* metal production it is also difficult to have patches of metal-free gas so that population III stars can continue to form. If instead we assume that most metals are ejected from the galaxy haloes into the IGM, we find (assuming $X = 3$) that the IGM mean metallicity would be

$$Z_{\text{IGM}} = 3g \times 10^{-3} Z_{\odot} \left(\frac{\tau_e}{0.1} \right). \quad (13)$$

But this value is about ten times larger than the estimated mean metallicity $Z \simeq 2 \times 10^{-4} Z_{\odot}$ of mildly overdense regions in the IGM at redshift $z \simeq 3$ (Schaye et al. 2003). It seems therefore that we need to find a mechanism to hide most heavy elements. If metal enriched gas remains highly inhomogeneous in the ISM, population III stars could continue to form for a while, together with normal stars. This scenario is not implausible but, because of the formation of some small-mass stars, the efficiency of UV emission will be reduced to $\epsilon_{\text{UV}} < 10^{-3}$ and reionisation would not occur by this process.

Let’s now relax the assumption that population III stars have the same yields as population II stars. The initial mass function and metal yields from population III stars are extremely uncertain¹ The simplest way to parametrise these uncertainties is to assume that a fraction, f_{BH} , of population III star mass and metals collapses onto BHs. The baryon fraction in seed BHs, $\omega_{\text{BH}} = f_{\text{BH}} f_*$, and the

¹ . Metal-free stars in the mass range $10 M_{\odot} < M_* < 130 M_{\odot}$ have reduced yields because, being more compact than population II stars, they are characterised by a large amount of heavy element fall-back onto the black hole remnant. Stars more massive than $260 M_{\odot}$ do not explode as SNe but rather collapse directly into a BH without exploding. On the other hand, stars with masses $130 M_{\odot} < M_* < 260 M_{\odot}$ provide the worst case for metal pollution and mechanical energy input. They explode as pair-instability SNe ($E_{51} \sim 10 - 100$), ejecting all of the metals without leaving any remnant and leaving a specific signature in the relative abundance distributions that has been sought for but not found (Venkatesan & Truran 2003).

metal production are given by

$$\omega_{\text{BH}} \sim f_{\text{BH}} 2 \times 10^{-4} \left(\frac{2 \times 10^{-3}}{\epsilon_{\text{UV}}} \right) \left(\frac{\tau_e}{0.1} \right), \quad (14)$$

$$Z \sim (1 - f_{\text{BH}}) 3g \times 10^{-3} Z_{\odot} \left(\frac{\tau_e}{0.1} \right). \quad (15)$$

An upper limit for the total mass of seed BHs can be estimated assuming that most of the mass in supermassive black holes (SMBHs) observed in the bulges of galaxies at $z = 0$ is built up from the merger of seed BHs. We estimate a baryon fraction in SMBHs, $\omega_{\text{BH,max}}$, from the BH-bulge mass relation (e.g., Kormendy & Richstone 1995) and from the estimated baryon fraction in spheroids, ω_{bulge} , at $z = 0$:

$$\omega_{\text{BH,max}} = \left(\frac{M_{\text{SMBH}}}{M_{\text{bulge}}} \right) \omega_{\text{bulge}} = (1 \pm 0.7) \times 10^{-4}.$$

We adopted the values $M_{\text{SMBH}}/M_{\text{bulge}} = (1.5 \pm 0.3) \times 10^{-3}$ (Gebhardt et al. 2000) and $\omega_{\text{bulge}} = (6.5 \pm 3)\%$ (Persic & Salucci 1992; Fukugita et al. 1998). This is an upper limit because a substantial fraction of the mass of SMBHs must be due to gas accretion to account for the luminosity of quasars. It is also possible, however, that a fraction of seed BHs is expelled from their host galaxies or does not end up in the observed population of SMBHs (Madau & Rees 2001). The recent discovery of several ultra-luminous X-ray sources (ULX) has been interpreted as evidence for intermediate-mass BHs (of about $100 M_{\odot}$). These objects could be relics of primordial BHs. Theoretical studies have shown that the expected luminosity function of accreting relic BHs in galaxies is consistent with observations of ULX source (Islam et al. 2003a,b). Since we do not know how much they contribute to the BH mass budget at $z = 0$ in the calculation presented here, we neglect their contribution. In any case, in paper II and paper III we will show that the upper limit on ω_{BH} adopted here is valid independently of the fate of the first BHs because it is constrained by limits on the observed γ -ray background. If we use the baryon fraction in SMBHs at $z = 0$, $\omega_{\text{BH,max}} = 10^{-4}$, as an upper limit for ω_{BH} in equation (14) and $Z_{\text{IGM}} = 2 \times 10^{-4} Z_{\odot}$ as an upper limit for the IGM metallicity given by $Z_{\text{IGM}} = \langle f_{\text{ej}} \rangle Z$, where $\langle f_{\text{ej}} \rangle$ is the fraction of metals ejected into the IGM and Z is from equation (15), we find:

$$1 - \frac{0.07}{g \langle f_{\text{ej}} \rangle} \left(\frac{\tau_e}{0.1} \right)^{-1} < f_{\text{BH}} < 0.5 \left(\frac{\epsilon_{\text{UV}}}{2 \times 10^{-3}} \right) \left(\frac{\tau_e}{0.1} \right)^{-1}.$$

We estimate that, if population III stars reionised the IGM to the value measured by WMAP ($\tau_e \sim 0.17$), the mass fraction of population III stars that might collapse into BHs is $f_{\text{BH}} \sim 30\%$ and the metal yield of population III stars is less than half the “normal” value. This result is rather extreme but plausible if population III stars have masses $M_* > 260 M_{\odot}$ or if their explosion energy is $E_{51} < 1$. Using the same assumptions as before on the metal and BH budget, we find an upper limit on the Thomson optical depth

$$\tau_e < 0.05 \left(\frac{\epsilon_{\text{UV}}}{2 \times 10^{-3}} \right) + \frac{0.007}{g \langle f_{\text{ej}} \rangle}.$$

In conclusion, if the optical $\tau_e \sim 0.17$ of the IGM is due to ionising radiation from massive stars, we need to assume that most of the heavy elements synthesised in the stars are not ejected into either the ISM or IGM. Similar conclusions have been found in order to prevent IGM over-enrichment with heavy elements by population III stars, if they have to account for the observed near-infrared background excess after subtraction of ‘normal’ galaxies contribution (Bond et al. 1986; Shchekinov 1986; Santos et al. 2002; Salvaterra & Ferrara 2003).

Table 1. List of simulations with radiative transfer.

#	RUN	N_{box} h^{-1} Mpc	L_{box} h^{-1} Mpc	Mass Res. h^{-1} pc	Res. (com.) h^{-1} Mpc	Smaller galaxy	ϵ_*	$\epsilon_{\text{UV}} \langle f_{\text{esc}} \rangle$	F_{IMF}
1	64L1VM	64	1.0	3.15×10^5	976	3×10^7	0.1	10^{-3}	17
2	64L2VM	64	2.0	2.52×10^6	1952	2.5×10^8	0.1	10^{-3}	17
3	128L1VM	128	1.0	3.94×10^4	488	4×10^6	0.1	10^{-3}	17
4	128L2VM	128	2.0	3.15×10^5	976	3×10^7	0.1	10^{-3}	17
5	128L4VM	128	4.0	2.52×10^6	1952	2.5×10^8	0.1	10^{-3}	17
6	128L2VMb	128	1.0	3.15×10^5	976	3×10^7	0.1	10^{-3}	1

Parameter description. *Numerical parameters:* N_{box}^3 is the number of grid cells and L_{box} is the box size in comoving h^{-1} Mpc. The mass of the DM particles is listed in column four, the comoving spatial resolution in column five and the minimum DM mass of resolved galaxies (with at least 100 DM particles) is given in column six. *Physical parameters:* ϵ_* is the star formation efficiency, ϵ_{UV} is the ratio of energy density of the ionising radiation field to the gas rest-mass energy density converted into stars (depends on the IMF), $\langle f_{\text{esc}} \rangle$ is the escape fraction of ionising photons from the resolution element and F_{IMF} is a weighting parameter for the energy input and metal yields from SN explosions, that differs from unity if the IMF is not a standard Salpeter IMF (see § 3.2).

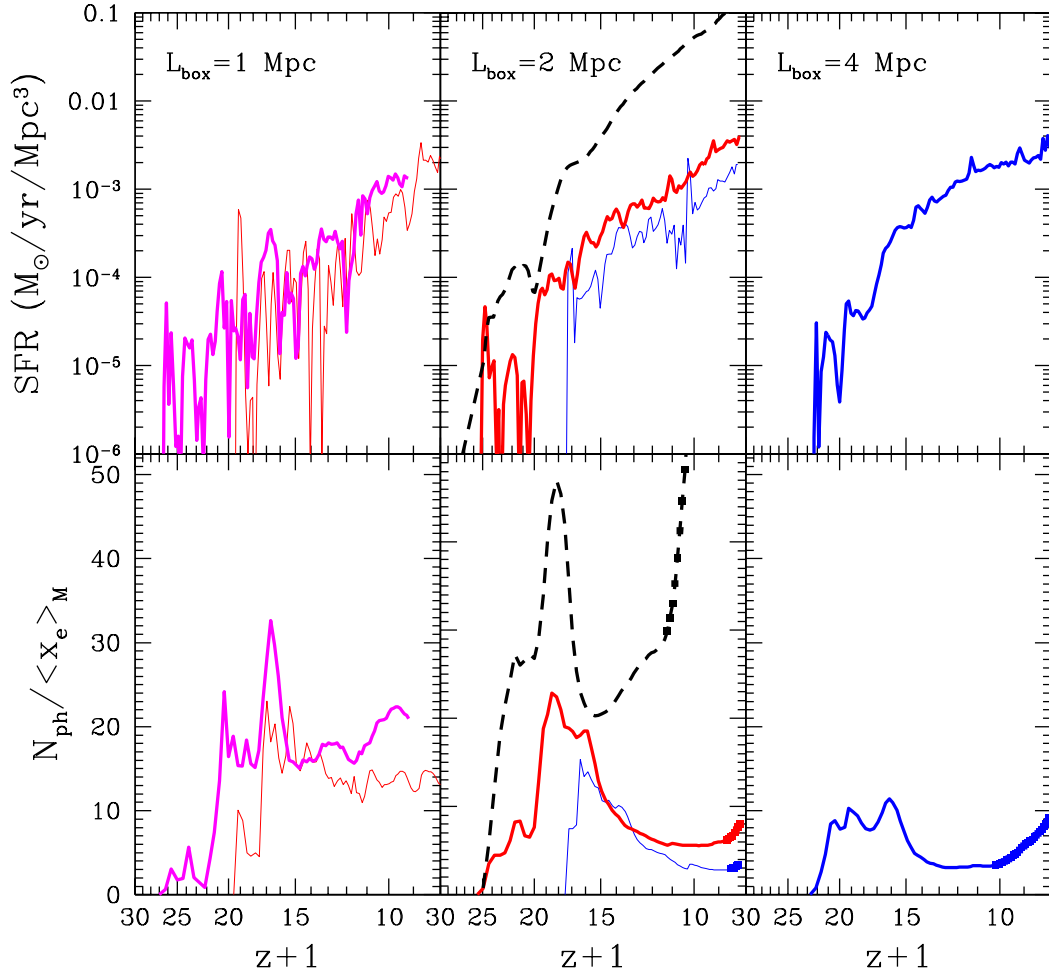


Figure 1. (top panels) Star formation rate as a function of redshift for the simulations in table 1. The thick lines refer to simulations with $N_{\text{box}} = 128$ and the thin lines refer to simulations with $N_{\text{box}} = 64$. All the simulations except 128L2VMb (thick dashed line) include strong feedback from SN explosions and differ only in box size. The $L_{\text{box}} = 1 h^{-1}$ Mpc simulation resolves small-mass galaxies in which star formation is strongly suppressed by SN explosions. We achieve convergence in both $L_{\text{box}} = 2$ and $L_{\text{box}} = 4 h^{-1}$ Mpc simulations, where the galaxies that dominate the SFR at $z > 10$ are numerically resolved. In simulation 128L2VMb we reduced the energy input from SN explosions by a factor of ten. The resulting SFR is about 20 times larger. Integrated number of ionising photons produced per free electron, $N_{\text{ph}} / \langle x_e \rangle$, as a function of redshift (bottom panels). The redshifts after reionisation are marked with points.

A very inefficient mixing of the ejecta with primordial gas is also a possible scenario. This would lead to the situation in which the high density regions, preferred for subsequent star formation, are contaminated by metals by more than the average amount but the metals are not incorporated into subsequent stars formed locally until after some delay. If the mechanism of metal ejection leads to metal exclusion from the star-forming high density regions, multiple generations of population III stars could form in the same galaxy and in neighbouring galaxies. In this scenario the gas metallicity and overdensity are anticorrelated. Numerical simulations fail to reproduce this anticorrelation but this could be a consequence of the insufficient numerical resolution and the badly understood physics of metal transport. As a consequence most metals would reside in the Lyman- α forest at high redshift. Observation of the metallicity in the Lyman- α forest and the metallicity in quasar host galaxies at $z \sim 3$ do not show anticorrelation of density and metallicity, but this scenario cannot at present be ruled out at high redshift.

Perhaps a more natural choice is to assume that most of the excess metals are locked inside intermediate-mass BHs. The recently discovered lower metallicity star HE0107-5240 (with $[\text{Fe}/\text{H}] = -5.3$) is iron deficient and carbon rich (Christlieb et al. 2002). The abundance pattern of HE0107-5240 can be explained by assuming that the gas has been enriched by a subluminous supernova explosion ($E_{51} \sim 0.3$) of a zero-metallicity star with a mass of $25 M_{\odot}$ (Umeda & Nomoto 2003). The iron metal yield is reduced because of fall-back into the central BH. The abundance pattern of HE0107-5240 is not compatible with yields from pair-instability SNe. To summarise, even with extremely optimistic assumptions concerning the UV efficiency of low metallicity stars we find that the only scenario capable of ionising the universe at high redshift is one in which a large fraction of the mass of population III stars collapses onto massive black holes.

3 COSMOLOGICAL SIMULATIONS

The results shown in the next section are based on numerical cosmological simulations that include radiative transfer and feedback from SN explosions. The code has been implemented to study stellar reionisation and the formation of the first galaxies that is self-regulated by radiative feedback effects in the early universe. The simulations were run on COSMOS, an SGI origins 38000 in DAMPT, University of Cambridge.

We adopt a concordance Λ CDM cosmological model with parameters: $\Omega_0 = 0.3$, $\Omega_{\Lambda} = 0.7$, $h = 0.7$ and $\Omega_b = 0.04$. The initial spectrum of perturbations has $\sigma_8 = 0.91$ and $n = 1$.

The effective emissivity is $\epsilon_{\text{UV}}^{\text{eff}} = \langle f_{\text{esc}} \rangle \epsilon_{\text{UV}}$. The value of ϵ_{UV} depends on the initial mass function (IMF) and the metallicity of the stellar population. Assuming a Salpeter IMF with star masses between $1 M_{\odot} \leq M_* \leq 100 M_{\odot}$, we have for population III (population II) stars $\epsilon_{\text{UV}} = 3 \times 10^{-4} (1.3 \times 10^{-4})$, $X = \bar{h}_p \nu / (13.6 \text{ eV}) = 2.47 (1.76)$ (e.g., Ricotti et al. 2002a). The quantity $\langle f_{\text{esc}} \rangle$ here is defined as the mean fraction of ionising radiation that escapes from the resolution element². Assuming

² Note that the definition of $\langle f_{\text{esc}} \rangle$ can create confusion. In numerical simulation, such as the ones presented in this work, $\langle f_{\text{esc}} \rangle$ is usually defined as subgrid physics, but in other works is defined as the mean fraction of ionising radiation escaping the galaxy haloes (e.g., the virial radii). The definition of $\langle f_{\text{esc}} \rangle$ and the definition of the clumping of the IGM are related and depend on how the outer edges of galaxies are defined. It is therefore dif-

a Salpeter IMF, $\langle f_{\text{esc}} \rangle$ must be in the range 20-50% in order to have reionisation at $z_{\text{rei}} \simeq 7$ (e.g., Benson et al. 2001; Gnedin 2000).

In this paper, as we are interested in determining an upper limit on τ_e , we adopt the maximum emissivity of ionising radiation $\epsilon_{\text{UV}}^{\text{max}}$ from stellar sources produced by thermonuclear reactions and $\langle f_{\text{esc}} \rangle = 0.5$. Assuming a constant emissivity is obviously not self-consistent since the metals ejected by population III stars eventually trigger the transition to the era when population II stars dominate the global star formation rate. In our simulations population III stars are dominant for long enough to fully reionise the IGM, but it should be kept in mind that, as noted above, due to metal enrichment, a complete reionisation by population III stars might never be achieved. In the next subsection we describe the main features of the code.

3.1 The Code

The simulations were performed with the ‘‘Softened Lagrangian Hydrodynamics’’ (SLH-P³M) code described in detail in Gnedin (1995). The cosmological simulation evolves collisionless DM particles, gas, ‘‘star-particles’’, and the radiation field in four frequency bins: optically thin radiation, H I, He I and He II ionising radiation fields. The radiative transfer is treated self-consistently (i.e., coupled with the gas dynamics and star formation) using the OTVET approximation (Gnedin & Abel 2001). The star particles are formed when the dense cooling gas in each resolution element sinks below the numerical resolution of the code. The code adopts a deformable mesh to achieve higher resolution in the dense filaments of the large scale structure. We solve the line radiative transfer in the H₂ Lyman-Werner bands for the background radiation. We include secondary ionisation of H and He, heating by Ly α scattering, detailed H₂ chemistry and cooling, and self-consistent stellar energy distribution of the sources (Ricotti et al. 2002a).

3.1.1 Feedback from SN explosions

We include the effects of SN explosions using the method discussed in Gnedin (1998). The current resolution of cosmological simulations does not allow numerical resolution of radiative shock fronts and the modelling of SN explosions from ‘‘first principles’’. A semi-analytic recipe has to be included at the sub-grid level. This treatment introduces new free parameters in the simulation and the results might depend on the model implemented. The approximation used to solve radiative transfer is instead much more reliable and has been shown, for simple test cases, to reproduce the exact solution. This is part of the reason why in our previous study on the formation of the first galaxies (Ricotti et al. 2002b) the effect of SN explosions was not included. In the present paper we find that, assuming a Salpeter IMF, the effect of SN explosions is not very important, so that omission in the earlier is justified. The main conclusions in Ricotti et al. (2002b) remain unchanged if we include SN feedback and the radiative feedback is strong enough (i.e., assuming a Salpeter IMF and $\langle f_{\text{esc}} \rangle \gtrsim 10\%$). However, in the current work assuming a top-heavy IMF, the SN energy injection has more dramatic effects and also affects galaxies with masses $M_* \gtrsim 10^9 M_{\odot}$.

difficult to compare predictions of different works (numerical and analytical) and estimate which are reasonable values to assume for the free parameter $\langle f_{\text{esc}} \rangle$. Nevertheless, $\langle f_{\text{esc}} \rangle$ cannot be treated purely as a freely adjustable parameter but has cosmological interest (e.g., Ricotti 2003a).

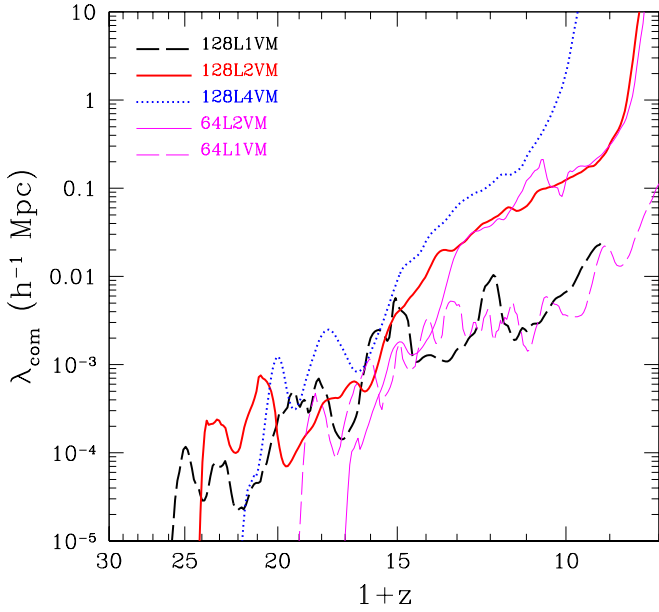


Figure 2. Comoving mean free path λ_{com} of H I ionising photons as a function of redshift. The size of H II regions before overlap is approximately equal to λ_{com} . Here we show λ_{com} for several simulations in table 1 to point out the effects of changing the box size and mass resolution.

3.2 Results

In table 1 we list the parameters adopted in the simulations. Here ϵ_* is the star formation efficiency of the adopted star formation law (Cen & Ostriker 1992): $d\rho_*/dt = \epsilon_*\rho_g/t_*$, where ρ_* and ρ_g are the stellar and gas density, respectively. The quantity t_* is the maximum of the local dynamical and the local cooling time. The escape fraction from a cell, $\langle f_{\text{esc}} \rangle$, is resolution-dependent. The parameter F_{IMF} is proportional to the mean metallicity yields and energy input by SN explosions of the stellar populations. This parameter is unity for a Salpeter IMF and population II stars. But $F_{\text{IMF}} > 1$ if the IMF is top-heavy and pair-instability SNe are dominant. Population III stars could have $F_{\text{IMF}} < 1$ if super-massive stars, that collapse directly into BHs without exploding as SNe, dominate the mass function.

3.2.1 Convergence study: $\langle f_{\text{esc}} \rangle$ and photoevaporation of minihaloes

We have run a set of simulations with box sizes $L_{\text{box}} = 1, 2$ and $4 h^{-1}$ Mpc and number of particles $N_{\text{box}}^3 = 64^3$ and $N_{\text{box}}^3 = 128^3$. The other parameters of the simulations, listed in table 1, are the same: we use the maximum efficiency of UV production allowed by thermonuclear reactions, $\epsilon_{\text{UV}}^{\text{max}} = 2 \times 10^{-3}$, and $\langle f_{\text{esc}} \rangle = 0.5$. We include the effect of SN explosions with an energy input and metal production 17 times the value for a Salpeter IMF. This is a reasonable assumption for a top-heavy IMF, if pair-instability SNe are important. But, given the uncertainties in the energy of SN explosions and on the IMF of population III stars, a scenario is also plausible in which population III stars collapse directly into BHs or produce subluminal SN explosions ejecting few metals. We explore this second scenario running a simulation with box size

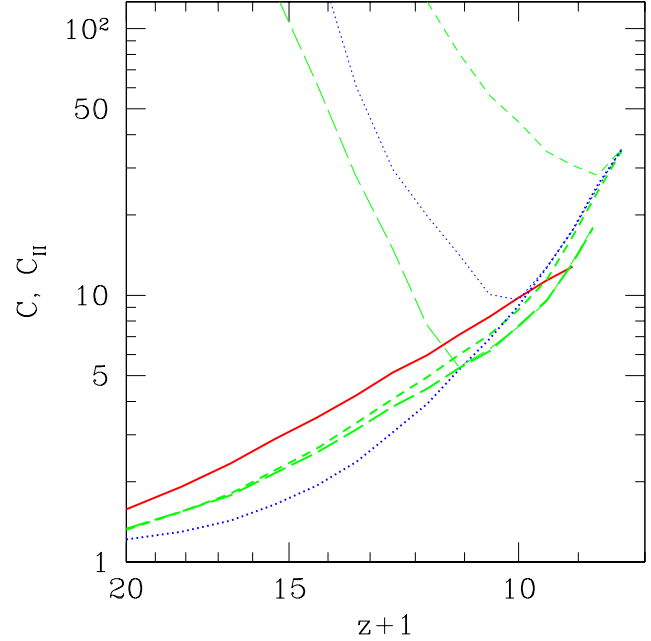


Figure 3. Clumping factor of the IGM, C (thick lines), and inside H II regions, $C_{\text{H II}}$ (thin lines), as a function of redshift. The solid, dashed and dotted lines show the clumping factor, C , for the strong SN feedback simulations with $N_{\text{box}} = 128$ and $L_{\text{box}} = 1, 2$ and $4 h^{-1}$ Mpc, respectively, listed in table 1. The long-dashed lines refer to the $L_{\text{box}} = 2 h^{-1}$ Mpc simulation with weak SN feedback.

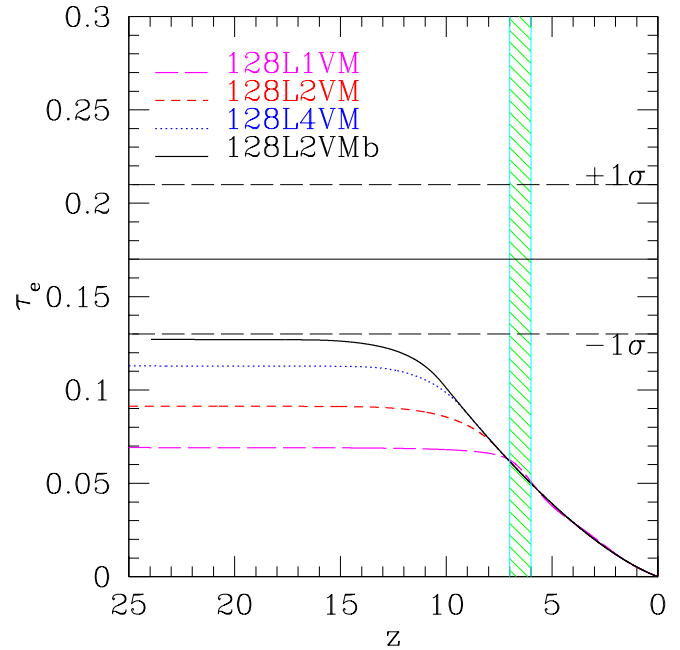


Figure 4. Optical depth to Thomson scattering, τ_e , as a function of redshift for the simulations with $N_{\text{box}} = 128$ listed in table 1. The horizontal lines show the best value of τ_e and 1σ confidence limits from WMAP (Kogut et al. 2003). The vertical band indicates the redshift probed by the furthest quasars found by the SLOAN survey.

$L_{\text{box}} = 2$ (128L2VMb in table 1) with reduced energy input and metal ejection ($F_{\text{IMF}} = 1$).

In the top panels of Fig. 1 we show the global star formation rate (SFR) as a function of redshift. In each panel, from left to right, we show simulations with box size $L_{\text{box}} = 1, 2$ and $4 h^{-1}$ Mpc. The thick lines show the $N_{\text{box}} = 128$ simulations and the thin lines the $N_{\text{box}} = 64$ simulations. The simulation with weak feedback is shown in the central panel with a dashed thick line. In the high-resolution $L_{\text{box}} = 1 h^{-1}$ Mpc simulation we resolve star formation in galaxies with masses $M_{\text{dm}} \gtrsim 3.94 \times 10^6 h^{-1} M_{\odot}$ (see Ricotti et al. 2002a). But, because of the strong feedback from SN explosions, star formation in the small-mass galaxies is suppressed. This can be seen comparing the top left panel to the simulations with larger box sizes and lower mass resolution. In the larger box simulations the first stars form later but the SFR quickly converges to the same value. The SFRs in the $L_{\text{box}} = 2$ and $L_{\text{box}} = 4 h^{-1}$ Mpc box are almost identical. At $z \sim 7$ the global SFR is $3 \times 10^{-3} M_{\odot} \text{yr}^{-1} h^{-1} \text{Mpc}^{-3}$. This value is still very small when compared to $\text{SFR} \sim 0.1 M_{\odot} \text{yr}^{-1} h^{-1} \text{Mpc}^{-3}$, estimated from observations at $z \sim 4 - 5$ (Lanzetta et al. 2002).

In the bottom panels of Fig. 1 we show the integrated number of ionising photons per free electron, $N_{\text{ph}}/\langle x_e \rangle$, as a function of redshift. The redshifts after reionisation (*i.e.*, $\langle x_e \rangle > 0.9$) are marked with points. The simulations shown are the same as in the top panels. At the redshift of reionisation the quantity N_{ph} measures the number of recombinations per baryon. If recombinations are negligible, N_{ph} is unity. From the plots it appears that the recombinations in the $N_{\text{box}} = 64$ simulations (thin lines) are always underestimated with respect to the simulations with higher mass resolution $N_{\text{box}} = 128$ (thick lines). We see that in the smaller scale boxes, which have higher mass resolution, and hence allow for lower mass halo formation, the integrated number of ionising photons produced per free electron required to reionise the IGM is larger. This number initially increases as the Strömgen spheres are finding their way through the denser regions surrounding the ionising sources. When the volume filling factor of the H II regions is larger, the ionisation fronts propagate mostly in the underdense regions and the integrated mean number of recombinations per baryon, $N_{\text{ph}}/\langle x_e \rangle$, decreases to less than 10. In the left panel the H II regions never break out of the dense filaments, because of the bursting mode of star formation in small-mass galaxies and the absence of large ones in the small box. Because of the self-limiting nature of the stellar feedback, as already found by Ricotti et al. (2002b), small-mass galaxies are not able to reionise the IGM. By comparing the middle and right panels we see that the integrated mean number of recombinations per baryon at the redshift of reionisation (marked by the first dot) is lower for the larger box size, that has lower mass resolution. This number is the same for simulations that have the same mass resolution (*e.g.*, the thin line in the middle panel and the thick line in the right panel).

We have shown that the integrated number of recombinations at the redshift of reionisation depends on the mass resolution of the simulation. This means that low resolution simulations might underestimate the clumping factor inside the H II regions (*cf.*, Fig. 3) or overestimate the mean value of $\langle f_{\text{esc}} \rangle$. Resolving small-mass haloes, that are photoevaporated during cosmic reionisation consuming a fraction of the ionising photons, may also be important to achieve a convergent value of τ_e (Shapiro & Raga 2000; Haiman et al. 2001; Barkana & Loeb 2002). We also note that the bursting mode of star formation in small-mass galaxies increases the number of recombinations and thus increases the number of ionising photons needed to reionise the IGM.

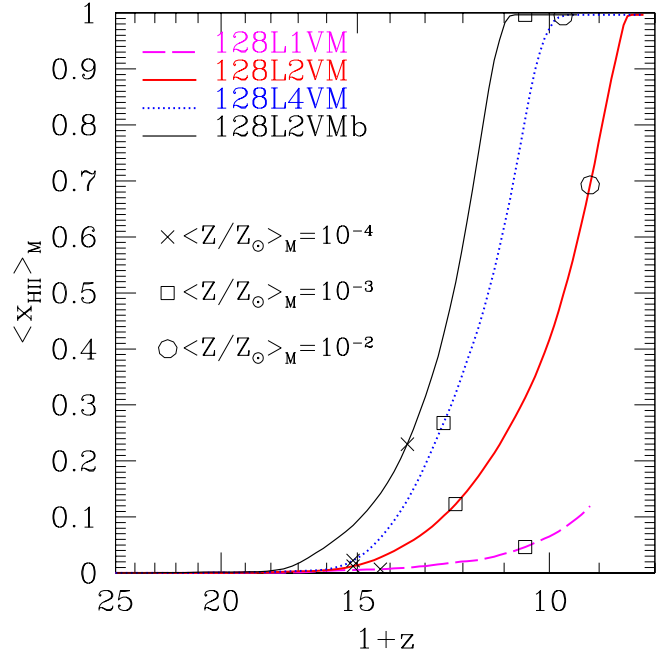


Figure 5. Hydrogen ionisation fraction as a function of redshift for the simulations with $N_{\text{box}} = 128$ listed in table 1. The circles, squares and crosses show the redshift at which the mass weighted mean metallicity in each simulation is $Z = 10^{-2}$, 10^{-3} , and $10^{-4} Z_{\odot}$, respectively.

In Fig. 2 we show the comoving mean free path λ_{com} of H I ionising photons as a function of redshift for the simulations in table 1 with strong feedback from SN explosions. The simulations with $L_{\text{box}} = 2 h^{-1}$ Mpc and $L_{\text{box}} = 4 h^{-1}$ Mpc have approximately the same SFR but in the larger box reionisation (defined as the redshift at which λ_{com} increases steeply) happens much earlier: $z_{\text{rei}} \approx 7.5$ in the $L = 2 h^{-1}$ Mpc run and $z_{\text{rei}} \approx 9.5$ in the $L_{\text{box}} = 4 h^{-1}$ Mpc run. The two $L_{\text{box}} = 2 h^{-1}$ Mpc simulations with different mass resolutions ($N_{\text{box}} = 64$ and 128) reionise the IGM at the same redshift even if the SFR is half in the smaller resolution simulation. This effect can also be seen comparing the $L_{\text{box}} = 1 h^{-1}$ Mpc simulations with the others. These results show that, even if we do not need to resolve small-mass haloes to have a convergent global SFR, we do need a high mass resolution or otherwise the optical depth to electron Thomson scattering will be overestimated due to neglect of recombination in high density regions.

3.2.2 Strong and weak SN feedback

In Fig. 4 we show the optical depth to Thomson scattering, τ_e , as a function of redshift for the simulations with $N_{\text{box}} = 128$ in table 1. In Fig. 5 we show the hydrogen ionisation fraction as a function of redshift for the same simulations. If we define z_{rei} as the redshift at which the hydrogen ionisation fraction is 90%, we find $z_{\text{rei}} = 7.5$ for the $L = 2 h^{-1}$ Mpc simulation with strong SN feedback and $z_{\text{rei}} = 10$ for the simulation with weak SN feedback. For the same simulations the optical depths are $\tau_e = 0.09$ and $\tau_e = 0.13$, respectively. These optical depths are considerably larger than expected for a sudden reionisation at z_{rei} . This is because the duration of reionisation, from the redshift where the mass-weighted mean hydrogen fraction is 10%, to complete reionisation, is quite long. We

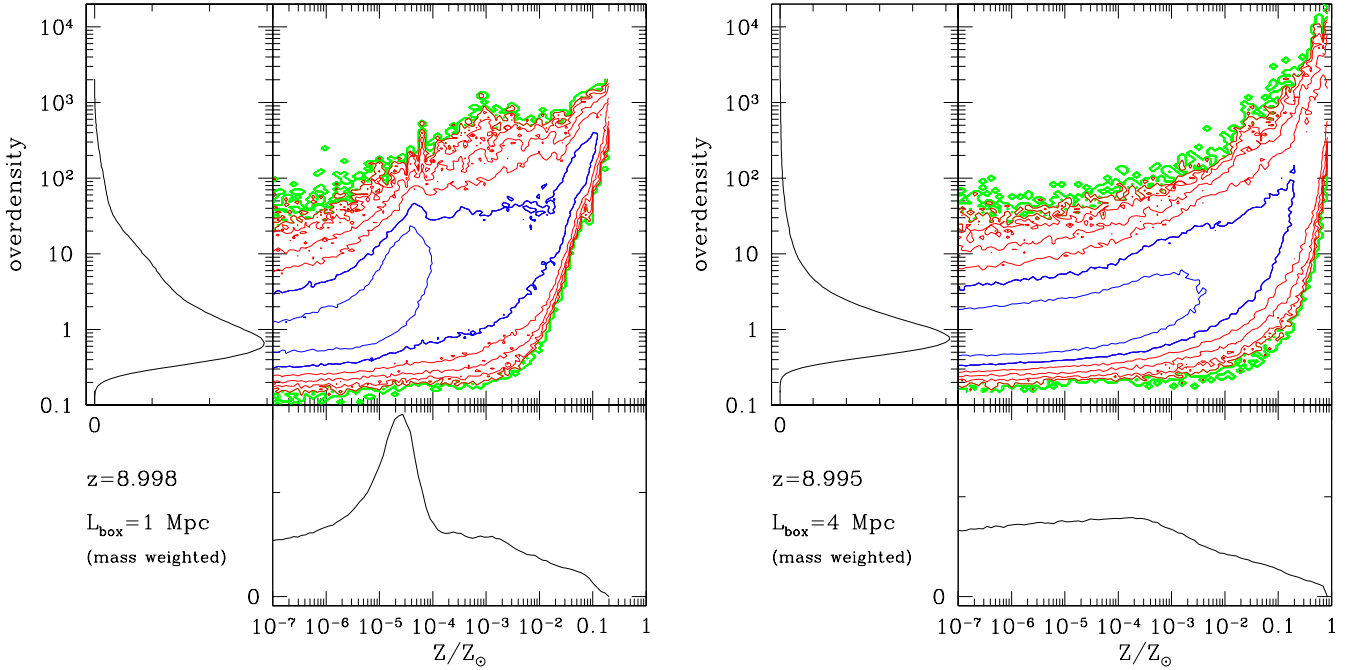


Figure 6. (left) Mass weighted metallicity-overdensity distribution for the simulation 128L1VM at redshift $z = 9$. The presence of metal-enriched wind with $Z \sim 10^{-4} Z_{\odot}$, produced by SN explosions in small-mass galaxies ($M > 4 \times 10^6 M_{\odot}$), is evident in both the metallicity distribution and density distribution. (right) The same as in the left panel but for the simulation 128L4VM. The galaxies resolved in this simulation are less affected by SN explosions because of their larger masses ($M > 2.5 \times 10^8 M_{\odot}$).

find approximately $\Delta z_{\text{rei}}/z_{\text{rei}} \sim 50\%$. The maximum $\tau_e \lesssim 0.13$ found for the $L_{\text{box}} = 2 h^{-1} \text{ Mpc}$ simulation is obtained for the case when SN feedback is not important. But this condition is not sufficient. The maximum optical depth, $\tau_e \simeq 0.13$, can be achieved only if the metallicity of the gas in star forming regions remains lower than a critical value. In the next section we show that this requirement puts strong constraints on the yield that population III stars may have in order to contribute to the IGM reionisation.

In summary, we do not achieve convergence for the simulations with strong feedback. Rare massive galaxies in this case contribute to the global SFR, because star formation in the smaller ones is suppressed by SN explosions. For this reason we need a box size of at least $L_{\text{box}} = 4 h^{-1} \text{ Mpc}$ to achieve a converged estimate for the SFR. But when we increase the box size the mass resolution becomes too small and we underestimate the clumping of the IGM (*i.e.*, the number of recombinations). For this reason, even if the SFR has converged, τ_e is likely to be overestimated because of the too low recombination rate in the $L_{\text{box}} = 4 h^{-1} \text{ Mpc}$ box. The $L_{\text{box}} = 2 h^{-1} \text{ Mpc}$ run instead gives a better estimate of τ_e because the underestimated clumping of the IGM is compensated by the slightly underestimated SFR. This can be seen by comparing the two $L_{\text{box}} = 2 h^{-1} \text{ Mpc}$ runs with 64^3 and 128^3 particles in the middle panels of Fig. 1: in the low resolution run the number of recombinations (bottom panel) and the SFR rate are underestimated (top panel). Fortunately these two effects almost cancel each other and, even if the low resolution simulation (thin lines) is not convergent, we did get an estimate of the redshift of reionisation (marked by the last dot in the bottom panel) and τ_e that is about the same as in the higher resolution simulation (thick lines).

For the weak feedback case we should be close to convergence since we can safely use the smaller box. In this case the SFR is large enough that the contribution from rare massive galaxies is

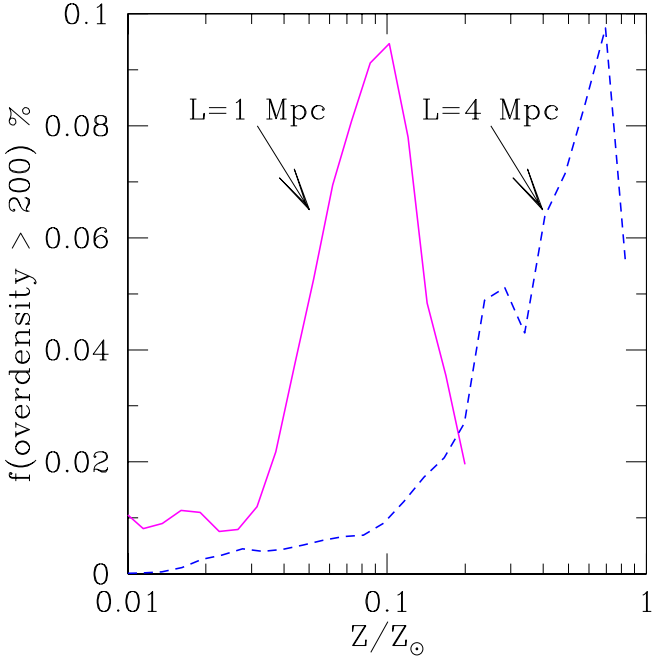
negligible. Unresolved small-mass galaxies do not contribute substantially to the SFR. Ideally, we need larger mass resolution to be sure that we are not underestimating recombinations. Note that $\langle f_{\text{esc}} \rangle$ is defined as the fraction of ionising photons that escapes from the resolution element. Therefore, by definition, it is resolution dependent and as we increase the resolution of the simulations its value should approach unity. We would use $\langle f_{\text{esc}} \rangle = 1$ if we could perfectly resolve galaxies down to the star forming regions in the ISM. Note that by definition, the effective clumping factor of the IGM is complementary to $\langle f_{\text{esc}} \rangle$, in the sense that it accounts for all the recombinations produced in regions larger or equal to the resolution element.

3.2.3 Metal enrichment

The circles, squares and crosses in Fig. 5 show the redshift at which the mass weighted mean metallicity in each simulation is $Z = 10^{-2}, 10^{-3}$, and $10^{-4} Z_{\odot}$, respectively. The volume weighted mean metallicities (not shown here) are ten times smaller than the mass weighted mean for both the simulations with strong and weak SN feedback. This means that most metals are located in overdense regions. This can be better seen in Fig. 6, where we show the mass weighted metallicity distribution as a function of the overdensity for the simulation 128L1VM with $L_{\text{box}} = 1 h^{-1} \text{ Mpc}$ (left) and 128L4VM $L_{\text{box}} = 4 h^{-1} \text{ Mpc}$ (right). In both simulations the mean metallicity increases with the overdensity. There is some scatter around the mean but at overdensities larger than 200 most of the gas has metallicity $Z \sim 0.1 - 0.01 Z_{\odot}$ (*cf.*, Fig. 7). These values are about ten times larger than the mass-weighted mean metallicities at the same redshift (or a hundred times the volume-weighted mean metallicities). Similar results were found by Cen & Ostriker (1999). If $Z_{\text{cr}} \simeq 10^{-4} - 10^{-5}$ is the critical metallicity at which

Table 2. Results of simulations with radiative transfer.

#	RUN	log f_*	log f_*	τ_e	z_{rei}	N_{ph}	log $\langle Z/Z_\odot \rangle$ at $z = 9$		
		at $z = 15$	at $z = 10$				volume weighted	mass weighted	$1 + \delta > 200$
3	128L1VM	-5.70	-5.00	0.07	-	-	-4.00	-2.70	-1.17
4	128L2VM	-5.70	-4.70	0.09	7.5	6.5	-3.52	-2.22	-0.66
5	128L4VM	-5.70	-4.53	0.11	8.7	3.4	-3.40	-2.10	-0.38
6	128L2VMb	-4.70	-3.22	0.13	9.9	30	-4.00	-2.70	-1.11

**Figure 7.** Metallicity distribution of the gas mass fraction with overdensity larger than 200 at redshift $z = 9$. The solid line refers to the simulation with box size $L_{\text{box}} = 1 \text{ h}^{-1} \text{ Mpc}$ and the dashed line to the simulation with box size $L_{\text{box}} = 4 \text{ h}^{-1} \text{ Mpc}$.

population II stars dominate over population III stars, it is quite clear from Fig. 5 that reionisation by population III stars cannot be completed in any of our simulations. Since stars are formed in overdense regions where the metallicities are larger, population III stars can not be important for reionisation unless their yield is much smaller than assumed here or the metals do not mix efficiently with metal-free gas. Note that we require a factor of 10^3 reduction in either yield or mixing efficiency to keep the metallicity below the level required for production of population III stars (*cf.*, Fig. 7). While Fig. 7 implies that population III is probably not relevant to reionisation it is not intrinsically implausible or inconsistent with observations. The quasar broad line emission regions sample the high density gas in galaxies and the Sloan high redshift quasars ($z \sim 6$) already show a metallicity approaching solar values. This is consistent with the most relevant ($L_{\text{box}} = 4 \text{ h}^{-1} \text{ Mpc}$) curve in Fig. 7 and would remain so even if we allow for 50 % fall-back of metals onto black holes.

In the simulation with $L_{\text{box}} = 1 \text{ h}^{-1} \text{ Mpc}$, the presence of metal-enriched galactic winds with $Z \sim 10^{-4} Z_\odot$, produced by SN explosions in small-mass galaxies ($M > 4 \times 10^6 M_\odot$), is evident in both the perturbed metallicity distribution and density distribution (*cf.*, Fig. 6). In the $L_{\text{box}} = 4 \text{ h}^{-1} \text{ Mpc}$ simulation galactic outflows are not important. The galaxies resolved in this simulation, because

of their larger masses ($M_{\text{dm}} > 2.5 \times 10^8 M_\odot$), are less affected by SN explosions and feedback.

In table 2 we give the values of relevant quantities measured in our high resolution simulations with parameters listed in table 1. Here ω_* is the fraction of baryons in stars, z_{rei} is the Gunn-Peterson reionisation redshift and N_{ph} is the number of ionising photons per baryon emitted at the redshift of reionisation. We show the mean mass weighted and volume weighted metallicities. In the last column we list the mean mass weighted metallicity in regions with overdensities > 200 .

As noted in § 1, the simple estimate presented in that section for the number of ionising photons N_{ph} as a function of the optical depth τ_e ,

$$N_{\text{ph}} \sim 10 \left(\frac{\tau_e}{0.1} \right)^\alpha, \quad (16)$$

with $\alpha = 1$ (*cf.*, equation [6]), is not very accurate when compared to the simulations. A better agreement with the simulations can be obtained using instead $\alpha = 4$. The reason for this result is that the mean effective clumping factor inside the H II regions it is not constant with redshift as was initially assumed. Using $\alpha = 4$ and $g = 2$ in equation (13), the estimated IGM metallicity as a function of τ_e is in good agreement with the simulation results listed in table 2. Since in equation (13) we have assumed that all the metals are ejected from the galactic haloes we should compare τ_e (given in the third column) to the mass weighted metallicities (given in the seventh column).

4 SEMIANALYTIC SIMULATIONS

In this section we use a simple semianalytic model to study the reionisation history of the IGM. This model can be useful to study the dependence of reionisation history on the assumed cosmological model and parameters. The semianalytic model do not include the effects of radiative feedback, SN feedbacks and metal enrichment. It also uses the results of the numerical simulations on the clumping factor of the IGM. Given these assumptions and limitations (due to neglecting feedbacks) the results of the semianalytic models are in good agreement with the numerical simulations. For example, the value of $\tau_e = 0.13$ found in our numerical simulation with weak SN feedback (128L1VMb) is shown as a circle in Fig. 8. The corresponding value found in the semianalytic model, shown with a square, is about 15% larger.

4.1 The code

We implemented a semianalytic model to study reionisation, chemical evolution and re-heating of the IGM. The method to calculate the filling factor of H II regions and the SFR is the same as in Chiu & Ostriker (2000). But we also include X-ray ionisation of the IGM before complete overlap of the H II regions. Since in this paper we neglect the X-ray background, a full description of the code will be given in Appendix A of paper II. Here we only briefly

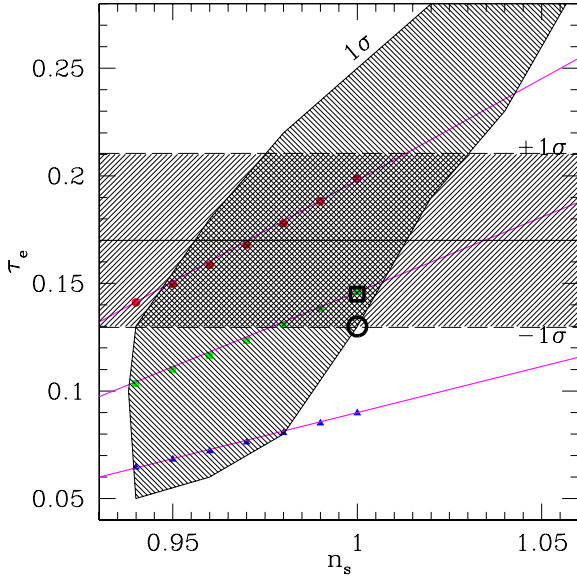


Figure 8. Optical depth to Thomson scattering, τ_e , as a function of the spectral index of initial density perturbations, n_s , computed from the semi-analytic code. Here σ_8 is calculated according to the amplitude of perturbations at $k = 0.05 \text{ h Mpc}^{-1}$ measured by WMAP. Each line from top to bottom shows $\tau_e(n_s)$ for effective efficiencies of UV emission $\epsilon_{UV}^{\text{eff}} = 10^{-2}, 10^{-3}$ and 10^{-4} , respectively. We show the 1σ confidence contour of $\tau_e - n_s$ (Spergel et al. 2003) and of τ_e (Kogut et al. 2003). The value of $\tau_e = 0.13$ found in our numerical simulation with weak SN feedback (128L1VMb) is shown as a circle. The corresponding value found in the semianalytic model, shown with a square, is about 15% larger.

summarise the main features of the semianalytic model. The mass function of DM haloes and their formation/merger rates are calculated using the extended Press-Schechter formalism. The SFR is assumed to be proportional to the formation rate of haloes. The effects of cooling and dynamical biases that depend on the mass of the haloes are taken into account. We consider the IGM as a two-phase medium: one phase is the ionised gas inside the H II regions and the other is the neutral or partially ionised gas outside. We solve the radiative transfer for the volume averaged specific intensity and we derive the specific intensity inside and outside the H II regions from their volume filling factor and separating the contribution from local UV sources and the background radiation from distant sources. We solve the time-dependent chemical network for eight ions (H, H⁺, H⁻, H₂, H₂⁺, He, He⁺, He⁺⁺), and the thermal evolution as a function of the gas density outside the H II regions. Given the clumping factor of fully ionised gas around the UV sources (taken from the SLH simulations) we evolve the filling factor, temperature and chemistry inside the H II regions. The following heating and cooling processes are included: collisional- and photo-ionisation heating, ionisation by secondary electrons, H, He, H₂ cooling, and Compton and adiabatic cosmological cooling. The rates are the same as in (Ricotti et al. 2001).

4.2 Dependence of τ_e on small-scales power

In this section we use the semianalytic code to study the dependence of τ_e on the cosmology (*e.g.*, Yoshida et al. 2003b,a). In particular we focus on models with a power spectrum of perturbations that differs in power at small-scales. Here we study the dependence

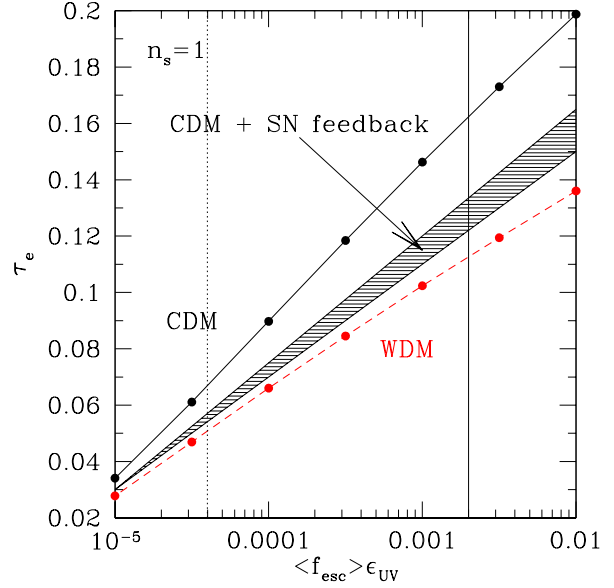


Figure 9. Optical depth to Thomson scattering, τ_e , as a function of the effective efficiency of UV emission $\langle f_{\text{esc}} \rangle \epsilon_{UV}$ for the CDM (solid) and a WDM (dashed) with particle mass 1.25 MeV cosmologies. We use a semi-analytic model with free parameters chosen to reproduce the results of the numerical simulation and the observed SFR at $z \sim 6$. Here feedback effects are neglected. We estimate that they would reduce τ_e by 20-25%, as shown in the shaded region for the CDM model, and leave the WDM model unaltered. The vertical solid line shows the maximum effective efficiency available from thermonuclear sources. Plausible (population II) models would shift it to the dotted line reducing τ_e to the level of 7-8% which is the value directly inferred by observations of quasar reionisation (Fan et al. 2003; Chiu et al. 2003) and is below the 2σ error bar of WMAP.

of τ_e on the slope of the initial power spectrum of perturbations for a CDM and warm dark matter (WDM) cosmology. The results presented in this section are intended to show the dependence of τ_e on the cosmological parameters, but they are not sophisticated enough to give a precise estimate of τ_e . The reader should keep in mind that in these models the most important feedback processes - those due to SNe - are neglected. In Fig. 8 we show τ_e as a function of the slope, n_s , of the power spectrum of initial density perturbations. We normalise the power spectrum according to the amplitude A at wave number $k = 0.05 \text{ h Mpc}^{-1}$ measured by WMAP (Verde et al. 2003). Consequently the variance σ_8 at $z = 0$ is determined by the value of n_s . We show the results for values of the product $\langle f_{\text{esc}} \rangle \epsilon_{UV} = \epsilon_{UV}^{\text{eff}} = 10^{-2}, 10^{-3}$ and 10^{-4} . The shaded contours show the 1σ confidence limits in the $\tau_e - n_s$ plane derived by the WMAP analysis of temperature fluctuations of the CMB (Spergel et al. 2003; Kogut et al. 2003). A small tilt, $n_s < 1$, suppresses the power on small scales delaying star formation in the first galaxies and the redshift of reionisation, as also found by Chiu et al. (2003). We find a linear relation between τ_e and the spectral index n_s :

$$\tau_e \simeq \tau_e(n_s = 1)4.54(n_s - 0.78),$$

where $\tau_e(n_s = 1)$ is the value of τ_e for $n_s = 1$. In Fig. 9 we show $\tau_e(n_s = 1)$ as a function of $\epsilon_{UV}^{\text{eff}}$ for the Λ CDM and Λ WDM cosmology. The optical depth τ_e increases exponentially with $\epsilon_{UV}^{\text{eff}}$:

$$\tau_e(n_s = 1) = a + b \log \left(\frac{\epsilon_{UV}^{\text{eff}}}{10^{-3}} \right),$$

where $a = 0.145(0.10)$ and $b = 0.055(0.036)$ for the Λ CDM (AWDM) cosmology. Our results roughly agree with a similar study by Chiu et al. (2003), but a precise comparison with their work is not possible since we adopt a constant effective efficiency of UV emission, $\epsilon_{\text{UV}}^{\text{eff}}$, while they adopt a time dependent effective efficiency.

The value of $\tau_e = 0.13$ found in our numerical simulation with weak SN feedback (128L1VMb) is shown as a circle in Fig. 8. The corresponding value found in the semianalytic model, shown with a square, is about 15% larger. This can be due to the finite resolution of the numerical simulation or the radiative and weak SN explosion feedbacks included in the numerical simulation but, considering these difference in the underlying assumptions, the agreement between the two methods is encouraging. In the numerical simulations including strong feedback, the SN explosion heating reduces the value of τ_e by 20 – 25% as compared to the weak feedback case.

We have also examined a warm dark matter model with our semianalytic set of calculations. If the strong SN feedback seen in the numerical simulations produces a similar reduction of τ_e in the semianalytic CDM model, we find that the warm dark matter model with particle mass 1.25 keV does, as expected, produce a lower τ_e but the effect is surprisingly small and estimated to be on 10 % for a given value of $\epsilon_{\text{UV}}^{\text{eff}}$ (cf., Fig. 9). The effect of SN explosions will leave the WDM model essentially unchanged because small-mass galaxies are not present in this model. The photoevaporation of minihaloes is expected to reduce τ_e in CDM models, but this effect is not present in WDM models.

5 CONCLUSION

We have used cosmological hydro-dynamical simulations with radiative and SN explosion feedback to study the reionisation of the IGM by population III stars. Simple calculations have been used to argue that a large τ_e is difficult to achieve and is incompatible with low metal enrichment of the IGM/ISM if population III stars end their lives as pair-instability SNe or smaller-mass hypernovae. A semianalytic code is used to study the dependence of τ_e on cosmological parameters.

The main results from the cosmological simulations are summarised in the following points.

(i) It is very difficult or impossible to use stellar sources to reionise the universe at $\tau_e > 0.13$ given a maximum efficiency of ionising radiation production typical (extreme population III) of thermonuclear fusion reactions $\epsilon_{\text{UV}}^{\text{max}} = 2 \times 10^{-3}$ and $\langle f_{\text{esc}} \rangle = 0.5$. When feedback from SN explosions is included, the limited mass resolution of the cosmological simulations is not crucial for achieving convergence for the global star formation history in the first galaxies. However a larger box size is required because the galaxies that contribute mostly to star formation are those that are the most massive. Our studies of convergence indicate that increasing the mass resolution over what we utilised in the 128L2VM run (which gave $\tau_e = 0.13$) would not increase τ_e for models with SN feedback.

(ii) If metal production is normal (top-heavy IMF, or pair instability SNe or hypernovae), the mechanical energy input by SN explosions is about ten times larger than for Salpeter IMF. This produces strong outflows in galaxies with masses $M_{\text{dm}} \lesssim 10^9 M_{\odot}$, reducing their star formation and delaying reionisation to $z_{\text{rei}} < 10$.

(iii) If the ratio of metal to ionising photons from metal poor population III stars is normal, then metal enrichment of the ISM

prevents metal-poor stars from being produced for long enough to reionise the IGM. One requires a factor of 10^3 reduction of yield or efficiency of mixing to alter this conclusion.

(iv) The issues raised in the previous two points can be alleviated if most population III stars collapse into a BH without producing a large amount of metals. This solves the metal pollution problem making the epoch of population III star domination longer. And in this scenario the mechanical feedback from SN/hypernovae explosions would also be reduced.

(v) If metal poor stars are initially important, then the secondary production of ionising radiation due to BH accretion may be more important than the primary production.

(vi) As a byproduct of the semianalytic treatment we find that a warm dark matter model with particle mass 1.25 keV does, as expected, produce a lower τ_e , but the effect is surprisingly small, and estimated to be on 10 % for a given value of $\epsilon_{\text{UV}}^{\text{eff}}$.

(vii) If we (self consistently) neglect population III and have more normal population II star formation properties we derive a much lower τ_e of 0.07 – 0.08 consistent with other authors but inconsistent with WMAP results.

In conclusion, if the first stars were massive and most of the radiation escaped from the host galaxies, the increase of τ_e could be within the 1σ confidence limits of WMAP data. But these two conditions are not sufficient. The energy liberated by SN explosions and the metal yields would have to have been much smaller than expected. This requirement seems to agree nicely with one possible interpretation of the abundance pattern in the recently discovered most iron-deficient star, HE0107-5240, and other metal-poor but carbon-rich stars. Subluminous supernova explosions with $E_{51} \sim 0.3$ are characterised by a large fall-back on the central black hole and their ejecta are carbon rich and iron deficient. The gas, enriched in carbon and oxygen, can cool fast enough to produce a second generation of stars with abundance patterns similar to HE0107-5240 (Umeda & Nomoto 2003). In addition the abundance pattern of HE0107-5240 is not compatible with the yields from pair-instability SNe. An interesting suggestion is that the energy of a SN might be low if the BH remnant is not spinning, and large for spinning BHs. Note that these conclusions are true even if the first stars were not supermassive. Indeed, the abundance pattern of HE0107-5240 can be explained assuming a mass of 25 M_{\odot} for the SN progenitor which is roughly the mass indicated by Abel et al. (2002) calculation of “the first star”. An interesting consequence of this scenario is a copious production of rather massive BHs from the first stars. For this reason, the secondary radiation from accretion on seed BHs might be a more important source of ionising radiation than the primary radiation from the massive stars (see also, Madau et al. 2003). BH accretion quickly builds up an X-ray background that can keep the IGM partially ionised before the complete reionisation by stellar sources at $z \sim 7$. We investigate this scenario in separate papers (paper Ila and paper IIb).

ACKNOWLEDGEMENTS

M.R. is supported by a PPARC theory grant. Research conducted in cooperation with Silicon Graphics/Cray Research utilising the Origin 3800 supercomputer (COSMOS) at DAMTP, Cambridge. COSMOS is a UK-CCC facility which is supported by HEFCE and PPARC. M.R. thanks Martin Haehnelt and the European Community Research and Training Network “The Physics of the Intergalactic Medium” for support. The authors would like to thank Renyue Cen, Andrea Ferrara, Nick Gnedin and Martin Rees for

useful conversations and the anonymous referee for useful suggestions that improved the manuscript. M.R would like to thank Erika Yoshino for proofreading the manuscript and support.

REFERENCES

- Abel, T., Bryan, G. L., & Norman, M. L. 2002, *Science*, 295, 93
- Barkana, R., & Loeb, A. 2002, *ApJ*, 578, 1
- Bean, R., Melchiorri, A., & Silk, J. 2003, *Phys. Rev. D*, 68, 083501
- Becker, R. H., et al. 2001, *AJ*, 122, 2850
- Bennett, C. L., et al. 2003, *ApJS*, 148, 1
- Benson, A. J., Nusser, A., Sugiyama, N., & Lacey, C. G. 2001, *MNRAS*, 320, 153
- Bond, J. R., Carr, B. J., & Hogan, C. J. 1986, *ApJ*, 306, 428
- Bromm, V., Coppi, P. S., & Larson, R. B. 1999, *ApJ*, 527, L5
- Bromm, V., Ferrara, A., Coppi, P. S., & Larson, R. B. 2001, *MNRAS*, 328, 969
- Cen, R. 2003a, *ApJ*, 591, L5
- Cen, R. 2003b, *ApJ*, 591, 12
- Cen, R., & Ostriker, J. P. 1992, *ApJ*, 399, L113
- Cen, R., & Ostriker, J. P. 1999, *ApJ*, 519, L109
- Chiu, W. A., Fan, X., & Ostriker, J. P. 2003, *ApJ*, 599, 759
- Chiu, W. A., & Ostriker, J. P. 2000, *ApJ*, 534, 507
- Christlieb, N., et al. 2002, *Nature*, 419, 904
- Ciardi, B., Ferrara, A., & White, S. D. M. 2003, *MNRAS*, 344, L7
- Ciardi, B., Stoehr, F., & White, S. D. M. 2003, *MNRAS*, 343, 1101
- Couchman, H. M. P., & Rees, M. J. 1986, *MNRAS*, 221, 53
- Fan, X., et al. 2003, *AJ*, 125, 1649
- Fukugita, M., Hogan, C. J., & Peebles, P. J. E. 1998, *ApJ*, 503, 518
- Gebhardt, K., et al. 2000, *ApJ*, 539, L13
- Gnedin, N. Y. 1995, *ApJS*, 97, 231
- Gnedin, N. Y. 1998, *MNRAS*, 294, 407
- Gnedin, N. Y. 2000, *ApJ*, 535, 530
- Gnedin, N. Y., & Abel, T. 2001, *New Astronomy*, 6, 437
- Gnedin, N. Y., Ostriker, J. P., & Rees, M. J. 1995, *ApJ*, 438, 40
- Guedens, R., Clancy, D., & Liddle, A. R. 2002, *Phys. Rev. D*, 66, 43513
- Haiman, Z., Abel, T., & Madau, P. 2001, *ApJ*, 551, 599
- Hansen, S. H., & Haiman, Z. 2004, *ApJ*, 600, 26
- Islam, R. R., Taylor, J. E., & Silk, J. 2003a, *ArXiv Astrophysics e-prints*
- Islam, R. R., Taylor, J. E., & Silk, J. 2003b, *ArXiv Astrophysics e-prints*
- Kogut, A., et al. 2003, *ApJS*, 148, 161
- Kormendy, J., & Richstone, D. 1995, *ARA&A*, 33, 581
- Lanzetta, K. M., Yahata, N., Pascarella, S., Chen, H., & Fernández-Soto, A. 2002, *ApJ*, 570, 492
- Larson, R. B. 1998, *MNRAS*, 301, 569
- Leitherer, C., et al. 1999, *ApJS*, 123, 3
- Madau, P., & Rees, M. J. 2001, *ApJ*, 551, L27
- Madau, P., Rees, M. J., Volonteri, M., Haardt, F., & Oh, S. P. 2003, submitted (astro-ph/0310223)
- Madau, P., & Shull, J. M. 1996, *ApJ*, 457, 551
- Mateo, M. L. 1998, *ARA&A*, 36, 435
- Miralda-Escudé, J. 2003, *Science*, 300, 1904
- Nakamura, F., & Umemura, M. 1999, *ApJ*, 515, 239
- Nakamura, F., & Umemura, M. 2001, *ApJ*, 548, 19
- Oh, S. P., Cooray, A., & Kamionkowski, M. 2003, *MNRAS*, 342, L20
- Omukai, K. 2000, *ApJ*, 534, 809
- Omukai, K., & Palla, F. 2003, *ApJ*, 589, 677
- Ostriker, J. P., & Gnedin, N. Y. 1996, *ApJ*, 472, L63
- Persic, M., & Salucci, P. 1992, *MNRAS*, 258, 14P
- Ricotti, M. 2003a, *MNRAS*, 344, 1237
- Ricotti, M. 2003b, in *The IGM/Galaxy Connection: The Distribution of Baryons at z=0*, ASSL Conference Proceedings Vol. 281. Edited by Jessica L. Rosenberg and Mary E. Putman. Kluwer Academic Publishers, Dordrecht, 2003, p.193, 193
- Ricotti, M., Gnedin, N. Y., & Shull, J. M. 2001, *ApJ*, 560, 580
- Ricotti, M., Gnedin, N. Y., & Shull, J. M. 2002a, *ApJ*, 575, 33
- Ricotti, M., Gnedin, N. Y., & Shull, J. M. 2002b, *ApJ*, 575, 49
- Ricotti, M., & Ostriker, J. P. 2003, submitted, (astro-ph/0310331), (paper IIa)
- Ricotti, M., Ostriker, J. P., & Gnedin, N. Y. 2004, in preparation, (paper IIb)
- Salvaterra, R., & Ferrara, A. 2003, *MNRAS*, 339, 973
- Santos, M. R., Bromm, V., & Kamionkowski, M. 2002, *MNRAS*, 336, 1082
- Schaye, J., Aguirre, A., Kim, T., Theuns, T., Rauch, M., & Sargent, W. L. W. 2003, *ApJ*, 596, 768
- Schneider, R., Ferrara, A., Natarajan, P., & Omukai, K. 2002, *ApJ*, 571, 30
- Sciama, D. W. 1982, *MNRAS*, 198, 1P
- Shapiro, P. R., & Raga, A. C. 2000, in *Revista Mexicana de Astronomia y Astrofisica Conference Series*, 292
- Shchekinov, I. A. 1986, *Astrofizika*, 24, 579
- Sokasian, A., Yoshida, N., Abel, T., Hernquist, L., & Springel, V. 2003, *ArXiv Astrophysics e-prints*
- Somerville, R. S., & Livio, M. 2003, *ApJ*, 593, 611
- Spergel, D. N., et al. 2003, *ApJS*, 148, 175
- Uehara, H., Susa, H., Nishi, R., Yamada, M., & Nakamura, T. 1996, *ApJ*, 473, L95
- Umeda, H., & Nomoto, K. 2003, *Nature*, 422, 871
- Vandenberg, D. A., Stetson, P. B., & Bolte, M. 1996, *ARA&A*, 34, 461
- Venkatesan, A., & Truran, J. W. 2003, *ApJ*, 594, L1
- Verde, L., et al. 2003, *ApJS*, 148, 195
- Wada, K., & Venkatesan, A. 2003, *ApJ*, 591, 38
- Wyithe, J. S. B., & Loeb, A. 2003, *ApJ*, 588, L69
- Yoshida, N., Sokasian, A., Hernquist, L., & Springel, V. 2003a, *ApJ*, 598, 73
- Yoshida, N., Sokasian, A., Hernquist, L., & Springel, V. 2003b, *ApJ*, 591, L1